Transition from Microstrip Line to Ridge Empty Substrate Integrated Waveguide Based on the Equations of the Superellipse

David Herraiz [1], **Héctor Esteban** [1,*], **Juan A. Martínez** [2], **Angel Belenguer** [2], **Santiago Cogollos** [1], **Vicente Nova** [1] **and Vicente E. Boria** [1]

[1] Instituto de Telecomunicaciones y Aplicaciones Multimedia, Universitat Politècnica de València, Camino de Vera, s/n, 46022 Valencia, Spain; daherza@teleco.upv.es (D.H.); sancobo@dcom.upv.es (S.C.); vinogi@iteam.upv.es (V.N.); vboria@dcom.upv.es (V.E.B.)

[2] Departamento de Ingeniería Eléctrica, Electrónica, Automática y Comunicaciones, Universidad de Castilla-La Mancha, Escuela Politécnica de Cuenca, Campus Universitario, 16071 Cuenca, Spain; juanangel.martinez@uclm.es (J.A.M.); angel.belenguer@uclm.es (A.B.)

* Correspondence: hesteban@dcom.upv.es; Tel.: +34-619842369

Abstract: In recent years, multiple technologies have been proposed with the aim of combining the characteristics of traditional planar and non-planar transmission lines. The first and most popular of these technologies is the Substrate Integrated Waveguide (SIW), where rows of metallic vias are mechanized in a printed circuit board (PCB). These vias, together with the top and bottom metal layers of the PCB, form a channel for the propagation of the electromagnetic fields, similar to that of a rectangular waveguide, but through a dielectric body, which increases the losses. To reduce these losses, the empty substrate integrated waveguide (ESIW) was recently proposed. In the ESIW, the dielectric is removed from the substrate, and this results in better performance (low profile and easy manufacturing as in SIW, but lower losses and better quality factor for resonators). Recently, to increase the operational bandwidth (monomode propagation) of the ESIW, the ridge ESIW (RESIW) and a transition from RESIW to microstrip line was proposed. In this work, a new and improved wideband transition from microstrip line (MS) to RESIW, with a dielectric taper based on the equations of the superellipse, is proposed. The new wideband transition presents simulated return losses in a back-to-back transition greater than 20 dB in an 87% fractional bandwidth, while in the previous transition the fractional bandwidth was 82%. This is an increment of 5%. In addition, the transition presents simulated return losses greater than 26 dB in an 84% fractional bandwidth. For validation purposes, a back-to-back configuration of the new transition was successfully manufactured and measured. The measured return loss is better than 14 dB with an insertion loss lower than 1 dB over the whole band.

Keywords: substrate integrated waveguide; ridge waveguide; tapering structure; broadband; microwave devices

1. Introduction

The growing need for small microwave devices with integration capabilities in planar technologies and high performance prompted the creation of the substrate integrated waveguide (SIW) [1]. In the quest for increasing the performance, the empty substrate integrated waveguide (ESIW) was developed [2]. In the ESIW, the dielectric is removed, the walls are metalized, and the electromagnetic wave is confined by a bottom and top metal covers. The removal of the dielectric allows a significant reduction of the losses, with the drawback of increasing the overall size. Consequently, the wave

is propagated through the air. To validate this promising technology, some common microwave devices have been designed, manufactured, and measured. Some of these devices are filters [3,4], antennas [5–7], 90° hybrid directional couplers [8], circulators [9], and phase shifters [10].

All of the above devices need a transition to connect ESIW to planar technologies. Multiple transitions from microstrip line (ML) to ESIW have been designed with a different approach in the design, solving the matching problems and being functional despite the manufacturing tolerances [2,11–13]. However, these transitions have the disadvantage of being well matched in a limited frequency range (monomode propagation in ESIW), resulting in a fractional bandwidth (FBW) of approximately 42%. This fractional bandwidth may be insufficient for some broadband applications. Recently, a new microstrip line to ESIW transition that can achieve a higher fractional bandwidth (57%) has been proposed [14]. This transition is based on introducing a dielectric material inside the waveguide, which allows for a greater bandwidth, but with the drawback of increasing the losses. In this work, we aim to achieve larger fractional bandwidth than 57% without introducing dielectric and therefore increasing the losses.

In the ESIW, the fundamental mode TE_{10} is propagated in a similar way as in a standard rectangular waveguide. The frequency range in which this is the only mode that is propagating determines the usable bandwidth. With the intention of increasing the monomode bandwidth a ridge waveguide can be used. The ridge waveguide consists of a waveguide with one or more metallic ridges. These ridges produce a reduction in the frequency of the fundamental mode and a small increase in the frequency of the next higher order mode. Thus, a significantly larger monomode bandwidth is achieved. Therefore, a ridge waveguide with the same dimensions of a rectangular waveguide without ridge can work at lower frequencies. Conversely, a ridge waveguide can work at the same frequency as the conventional rectangular waveguide, but being smaller and less bulky.

This idea of a Ridge ESIW (RESIW) was first presented by Murad et al. [15], and a transition from microstrip line to a single RESIW (RESIW with only one ridge) that allows the use of most of the usable bandwidth was also proposed by Herraiz et al. [16]. This transition for a WR62 RESIW presents return losses greater than 20 dB in a fractional bandwidth (FBW) of 82%.

In this work, a thorough study of possible geometries of a ridge ESIW manufactured with standard Planar Circuit Board (PCB) machinery is performed with the purpose of assessing the pros and cons of using only one o more ridges, and/or using ridges with different cross sectional shapes, and selecting the best geometry with a compromise between monomode propagation bandwidth and ease of manufacturing. Next, a new wideband transition from microstrip line to single RESIW is proposed. This new transition is based in a wider ESIW section with a superelliptical dielectric taper, and it presents better return losses and a broader fractional bandwidth than the previous microstrip to single RESIW transition [16].

The work is structured as follows. Section 2 presents an exhaustive study of the possible geometries of the RESIW. Section 3 presents the transition and it is design procedure. The results of the simulated and measured prototype are presented in Section 4. Finally, the conclusions are discussed in Section 5.

2. RESIW cross Section Design

The ridge waveguides are a family of waveguides which are composed of one or several metallic ridges attached to the lower or upper walls of the waveguide [17]. The best known and studied ridge waveguides are the single and double ridge rectangular waveguides [18]. The metallic ridges allow a reduction of the cutoff frequency of the fundamental mode (TE_{10}), and an increase of the cutoff frequency of the first higher order mode (TE_{20}). Thus, a broader bandwidth can be achieved. In addition, the characteristic impedance of the fundamental mode (Z_0) is reduced [19].

In practice, by properly selecting the geometrical parameters of the single and the double ridge waveguides, similar bandwidths can be achieved with either one. Therefore, to reduce the complexity of the manufacture, the single RESIW is our focus of study. The use of the conventional manufacturing techniques of planar technologies allows the creation of this single RESIW simply by piling substrates

of the same height. This leads to an easy manufacture, but limits the freedom in the design of the ridge dimensions, as shown in Figure 1. The height of the ridge (h_r) is limited by the height of the substrate (h_s) and can only be a multiple of this height ($h_r = n\,h_s$, where n is the number of ridge layers). The only parameter of the ridge transversal section that can be chosen freely is the ridge width w_r.

(**a**) ESIW   (**b**) RESIW with one layer ($n = 1$)
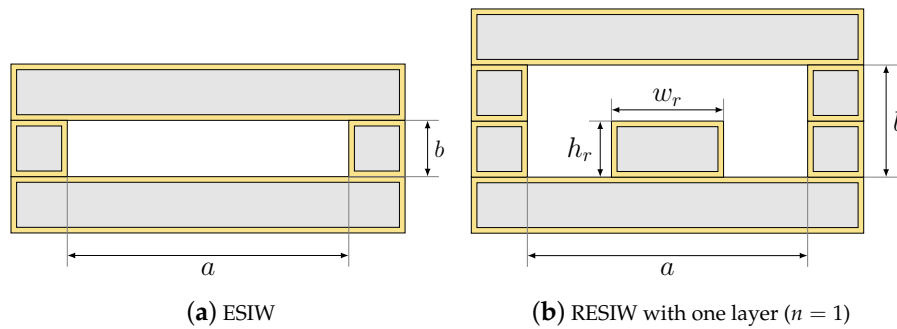
Figure 1. Cross sectional view of the ESIW and the ridge ESIW with one layer.

Appendix A shows that the one layer rectangular ridge ESIW proves to be the best compromise between maximizing the bandwidth and minimizing the related manufacturing cost and volume. Therefore, one-layer rectangular ridge ESIW is used in this work, where the waveguide width is $a = 15.7988$ mm (Standard waveguide WR-62) and the ridge width that maximizes the bandwidth is $w_r = 3.848$ mm.

3. Transition Design

The 3D view of the proposed topology for an improved wideband transition from microstrip line to one layer RESIW is shown in Figure 2a. The detailed layout with dimensions of the central (Figure 3a) and ridge layers (Figure 3b) of this transition is shown in Figure 3.
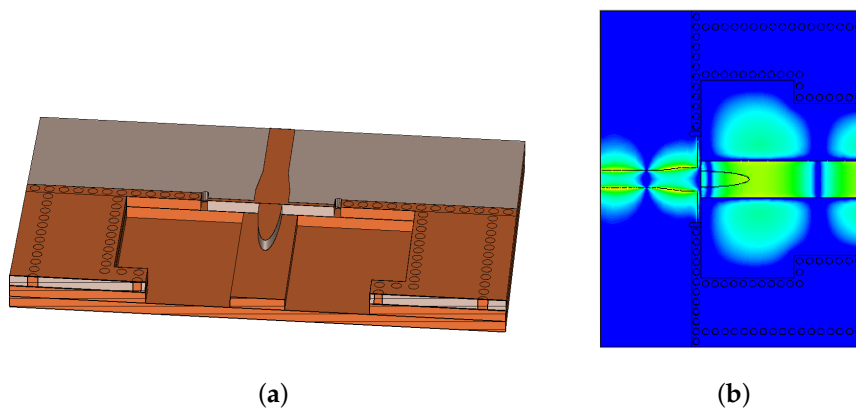

(**a**)   (**b**)

Figure 2. Structure of the proposed transition from microstripo to RESIW (**a**); and simulated field distribution for the central frequency (14 GHz) (**b**).

The transition is based in four elements in order to couple the fields and match the impedances of the input and output transmission lines. Since there is a large difference between the impedances of the microtrip (low impedance) and the RESIW (high impedance), the first element consists on a linear taper at the end of the microstrip line that gradually modifies the impedance of the microstrip line, thus easing the impedance matching with the RESIW. The second element of the transition is a widened RESIW section, placed at the beginning of the RESIW. This section is controlled with the parameters a_c (length) and b_c (width). This widening properly decreases the impedance of the RESIW,

so that the impedance matching with the microstrip is easier. This widening is manufactured in the central and in the ridge layer (see Figure 3a,b). The third element of the transition is an inductive iris of width w_{ti}, mechanized with rows of metallized via holes, that controls the coupling between the widened microstrip line and the widened RESIW. These three elements were already present in the previous version of the MS-RESIW transition [16] (see Figure 4a). In that previous transition, the matching was completed with the fourth element of the transition, which was a widening of the ridge at the beginning of the RESIW [16]. In this work, instead of using a widening of the ridge, the ridge has no widening and a dielectric taper is used in the central layer in order to better match the discontinuity between dielectric and air. The use of a dielectric taper, never used before in a transition from MS to RESIW, is inspired by the dielectric taper used in the transition from microstrip line to ESIW presented in [2] and improved in [11] (see Figure 4b). However, and conversely to what happens in the transition from MS to ESIW, the exponential dielectric taper provides poor results in the case of a transition from MS to RESIW. For that reason, in this work, we propose the use of the equations of the superellipse [20] for shaping the dielectric taper. This curve allows to explore an endless set of possible transition profiles, using just a few number of parameters and finding the optimum parameter values that provide with an excellent performance.
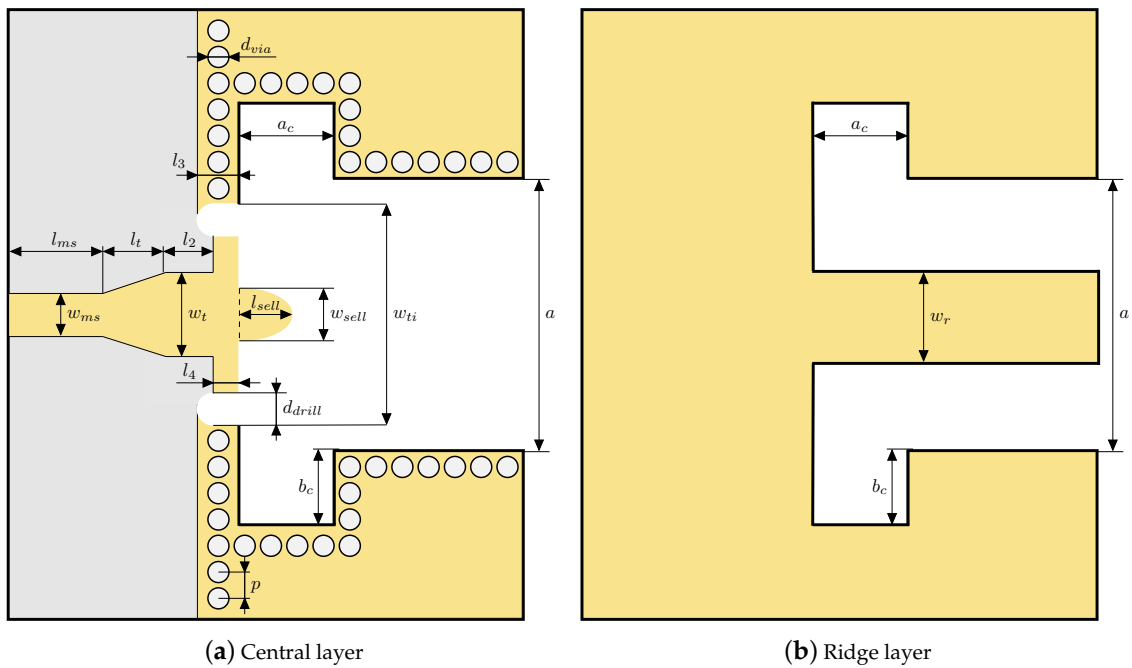

Figure 3. Layout of the microstrip line to RESIW transition proposed in this work. White represents empty spaces, gray represents dielectric body, and dark yellow represents copper surfaces.
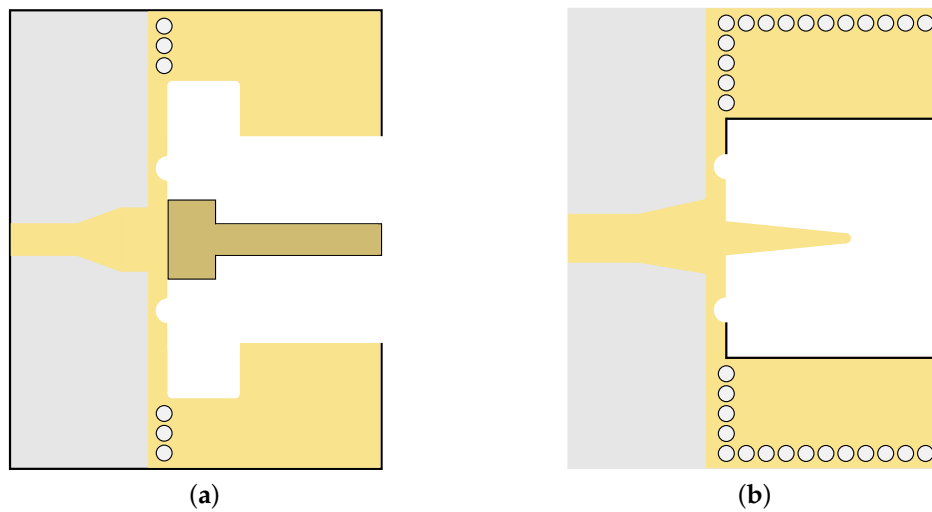
Figure 4. Previous transitions that inspired the transition presented in this work: (**a**) transition from MS to RESIW with widening of the ridge [16]; and (**b**) transition from MS to ESIW with exponential dielectric taper [11].

The equations of the superellipse have been used in several fields of the engineering, especially in architecture [21]. In the microwave field, they were used in [20] for defining a tapering impedance matching profile between two rectangular waveguides of different widths. The superellipse was first discussed in 1818 by Gabriel Lamé. It consists in a generalization of the equations of the ellipse, so that the ellipse is a particular case of the superellipse. The Cartesian equation of superellipse is,

$$\left(\frac{x}{a}\right)^m + \left(\frac{y}{b}\right)^m = 1 \tag{1}$$

where b and a are the semiaxes of the superellipse and m is the parameter controlling the overall shape of the ellipse. By properly selecting the value of m, a rectellipse ($m = 4$), an ellipse ($m = 2$), a straight line ($m = 1$), an astroid ($m = 2/3$), or other shapes can be obtained. The most known and studied values of m and its shapes are shown in Figure 5.
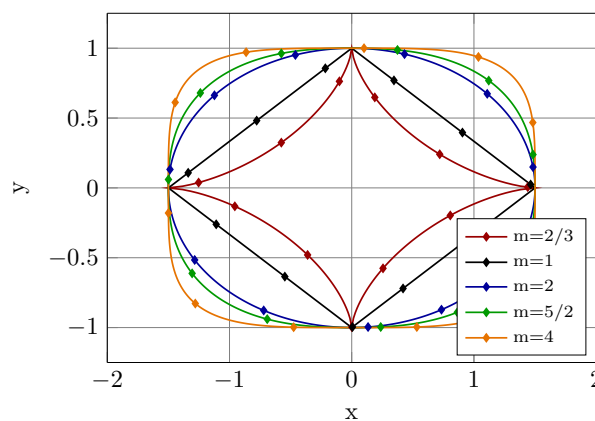

Figure 5. Superellipses with semiaxes $a = 1.5$ and $b = 1$ and different values for m.

With the aim of providing a better control over the shape of the superellipse, the equations can be further generalized as,

$$\left(\frac{x}{a}\right)^p + \left(\frac{y}{b}\right)^q = 1 \tag{2}$$

where p and q are real parameters that control the curvature of the superellipse in each dimension separately. Values of p less than one provide an inward curve with the y-axis. On the other hand,

values of p greater than one provide an outward curve with the y-axis. q controls the curvature in the x-axis. Extreme values for p or q (i.e., $p, q = 0$ or $p, q \rightarrow \infty$) produce a nose sharp curve or a blunt ellipse.

As shown in Figure 3, the idea is to create a dielectric taper whose semiaxes are l_{sell} and $w_{sell}/2$ and find the best possible values of p and q that provide the maximum impedance matching. Thus, Equation (2) is particularized for creating a dielectric taper that follows the following profile,

$$\left(\frac{x}{l_{sell}} \right)^p + \left(\frac{y}{\frac{w_{sell}}{2}} \right)^q = 1 \tag{3}$$

To accelerate the process of designing the proposed transition, it is convenient to find good initial values for the design parameters. Table 1 proposes expressions that provide with a good initial point that significantly reduces the computational cost of the optimization process. The expressions for the initial values of l_t, l_2, and w_t are extracted from [16]. The other expressions were obtained empirically, after designing several transitions at different frequencies and with different substrates. The value of λ_g for computing the initial expressions refers to the wavelength in the widened section of RESIW of width $a + 2b_c$.

Table 1. Initial expressions for the design parameters of the new MS to RESIW transition.

w_{ti}	w_t	l_t	a_c	b_c	w_{sell}	l_{sell}	l_2	p	q
$0.7a$	$0.2w_{ti}$	$\frac{\lambda_{ms}(f_0)}{4}$	$\frac{\lambda_g(f_0)}{2}$	$\frac{a}{6}$	$0.4w_r$	$\frac{\lambda_g(f_0)}{4}$	$\frac{l_t}{3}$	2	2

4. Results

To validate the transition, a back-to-back transition from a 50 Ω microstrip line to a RESIW with one ridge layer was designed, manufactured, and measured. A Rogers 4003C substrate with $h_r = 0.813$ mm, permittivity $\epsilon_r = 3.55$, and metal thickness $t = 35$ μm was used. The transition presents the same width of the standard WR-62 rectangular waveguide ($a = 15.7988$ mm). The expressions in Table 1 were applied to obtain initial values for the design parameters. Since the initial values were good enough, the optimum values were obtained after a quick and simple optimization process with the Neder-Mead Simplex algorithm of CST and the goal of maximizing the return loss. Table 2 shows the initial values of the design parameters and the final optimum values. It also shows the dimensions that are fixed and that do not need to be optimized.

Table 2. Dimensions of the designed MS to RESIW transition with Rogers 4003C substrate (in mm).

Fixed Parameters			Design Parameters								
			Initial	Final		Initial	Final		Initial	Final
p, l_3	1									
d_{via}	0.7	w_{ti}	11.059	10.014	l_{sell}	4.518	4.996	l_t	3.213	4.428
w_r	3.848	b_c	2.633	2.394	l_2	1.071	1.491	p	2.00	2.008
d_{drill}	0.5	a_c	11.836	9.629	w_t	2.211	2.446	q	2.00	2.016
w_{ms}	1.813	w_{sell}	1.528	1.635	l_4	0.3	0.329			

Figure 6 compares the simulated (with CST) reflection coefficient of the new transition presented here and the previous version presented in [16]. To assess the validity of the initial values of the design parameters, the reflection coefficient with these initial values is also plotted. It can be observed that the initial values provide a minimum return loss of about 12 dB in the whole band, which proves that the initial vales of Table 1 are a very good approximation to the final optimum values. Comparing the optimized transition proposed here and the previous transition presented in [16], it can be observed that the fractional bandwidth (calculated as the frequency range in which the return losses are greater than 20 dB divided by the central frequency, 14 GHz) is 82% with the previous transition of

Herraiz et al. [16] and 87% with the new transition, which supposes an increment of 5%. It can also be observed that the optimized new transition presents a return losses value greater than 26 dB from 8.7 to 20.5 GHz, which is a very good matching in a large bandwidth, thus proving its good performance in terms of simulated results.
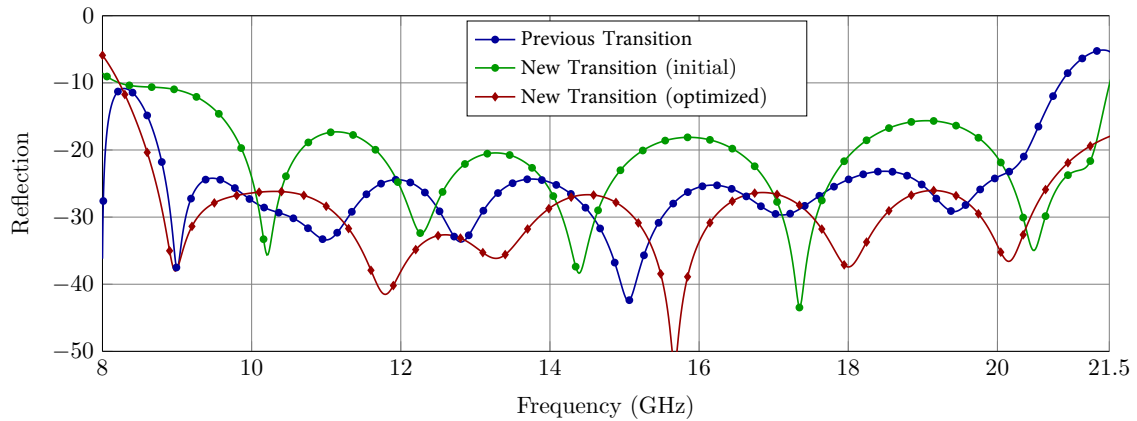
Figure 6. Return loss comparison between previous [16] and new version of the back-to-back transition from microstrip to RESIW. For the new transition, results of the design with initial values of the parameters and of the design with final optimized values are plotted.

The simulated insertion losses of the previous [16] and new transition are compared in Figure 7. Lossy metal and lossy dielectric are considered in the simulation with CST. It can be observed that the insertion losses of the new transition are lower than 0.6 dB in the whole band, whereas the insertions losses of the previous transition are greater than 1.2 dB.
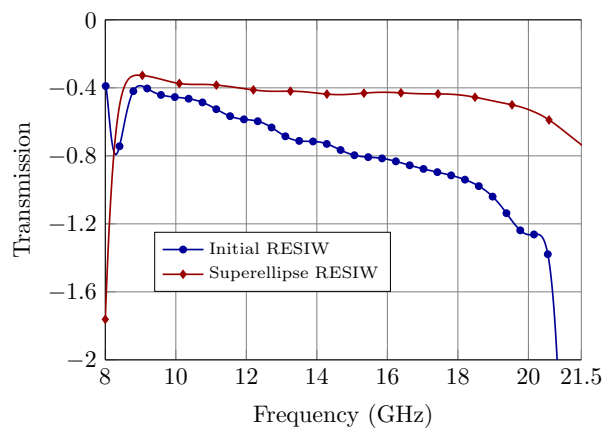
Figure 7. Insertion loss comparison between previous [16] and new back-to-back transition from microstrip to RESIW.

Therefore, the simulated results of the new version of the transition are better in terms of both insertion and return losses than the previous version of Herraiz et al. [16].

Figure 8 compares the return losses of the the back-to-back transition from microstrip to ESIW without ridge [11] and the new back-to-back transition from microstrip to RESIW presented here. There is an increment of 103% in the fractional bandwidth (return losses greater than 20 dB) with the new transition when compared with the transition from MS to ESIW without ridge, whose fractional bandwidth is 42%.
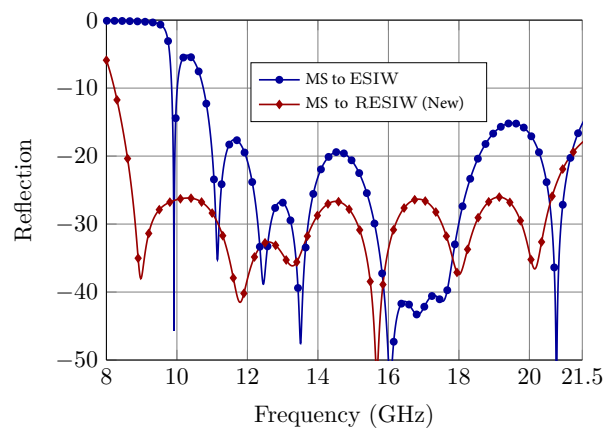
Figure 8. Return loss comparison between back-to-back transition from microstrip to ESIW [11] and this work.

The manufactured back-to-back prototype with the final design parameters of Table 2 is shown in Figure 9. Standard planar circuit manufacturing techniques (drilling, milling, and electrodeposition) were used to manufacture this prototype. Figure 10 compares the simulated and measured scattering parameters of the back-to-back transition prototype. The differences between measurement and simulation are mainly due to manufacturing tolerances and the effect of surface roughness on electrodeposited metallic surfaces. For the same cut, the tolerance of the laser beam is only 2 μm and for nonconsecutive cut is approximately 50 μm. The tolerance in the alignment of the layers is the same as of nonconsecutive cuts. The measurements include the effect of the transitions from coaxial to microstrip, which can be estimated in approximately 1 dB of additional insertion losses, and possibly some mismatch. Discounting the effect of the coaxial to microstrip connectors, the measured insertion loss of the back-to-back prototype is smaller than 1 dB, and the measured return loss is greater that 14.5 dB between 9 and 20.66 GHz, which corresponds to a fractional bandwidth of 83%. In [16], the return loss was 11 dB and the insertion loss was 1.5 dB between 8 and 20.5 GHz, which corresponds to a fractional bandwidth of 87% for a back-to-back transition with the same waveguide characteristics.

In comparison, the measured return and insertion losses of the new version of the transition are better than the previous one reported in [16].
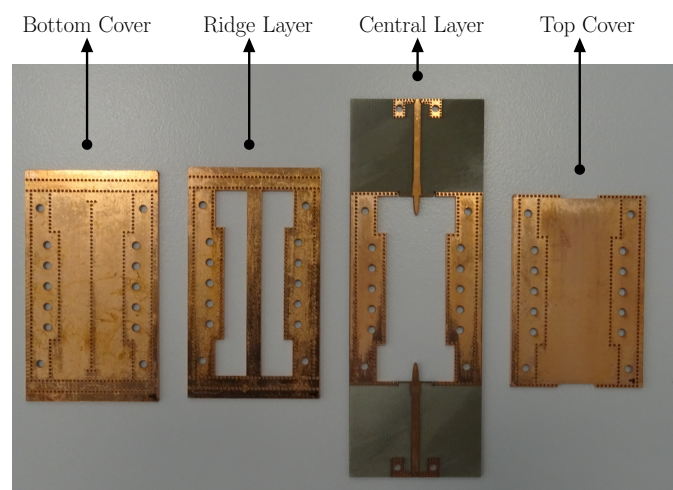

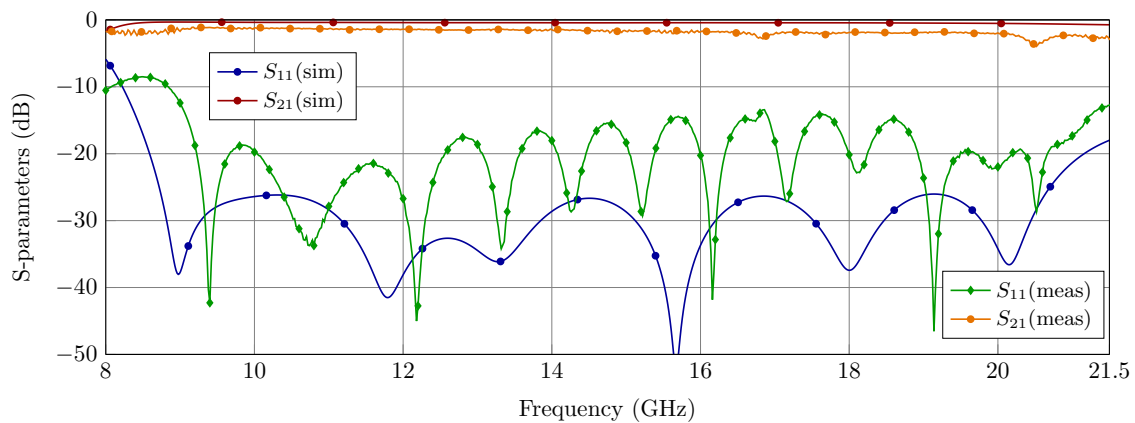**Figure 9.** Back-to-back manufactured prototype.

Figure 10. Comparison of measurements and simulations of the back-to-back transition prototype.

5. Conclusions

In this work, a novel transition from MS to RESIW based on the equations of the superellipse is proposed. A design procedure is presented and initial values for the design parameters are provided. The simulated reflection coefficient of a back-to-back transition is less than 20 dB in an 87% fractional bandwidth and less than 26 dB in an 84% fractional bandwidth. The measured return losses are greater than 14.5 dB and the insertion losses are lower than 1 dB in a 83% fractional bandwidth. The new wideband transition presents improved (simulated and measured) responses, with better return losses and lower insertion losses, when compared with the previous MS to RESIW transition.

Conflicts of Interest: The authors declare no conflict of interest. The founding sponsors had no role in the design of the study; in the collection, analyses, or interpretation of data; in the writing of the manuscript, and in the decision to publish the results.

Abbreviations

The following abbreviations are used in this manuscript:

SIW	Substrate Integrated Waveguide
PCB	Printed Circuit Board
ESIW	Empty Substrate Integrated Waveguide
RESIW	Ridge Empty Substrate Integrated Waveguide
FBW	Fractional Bandwidth
MS	Microstrip Line
CST	Computer Simulation Technology
WR	Rectangular Waveguide
RL	Return Loss

Appendix A. Study of Possible Geometries of a RESIW Crosssection

In this Appendix, an exhaustive study of the possible geometries of the RESIW is presented. Figure A1 shows the RESIWs transversal section that have been studied.
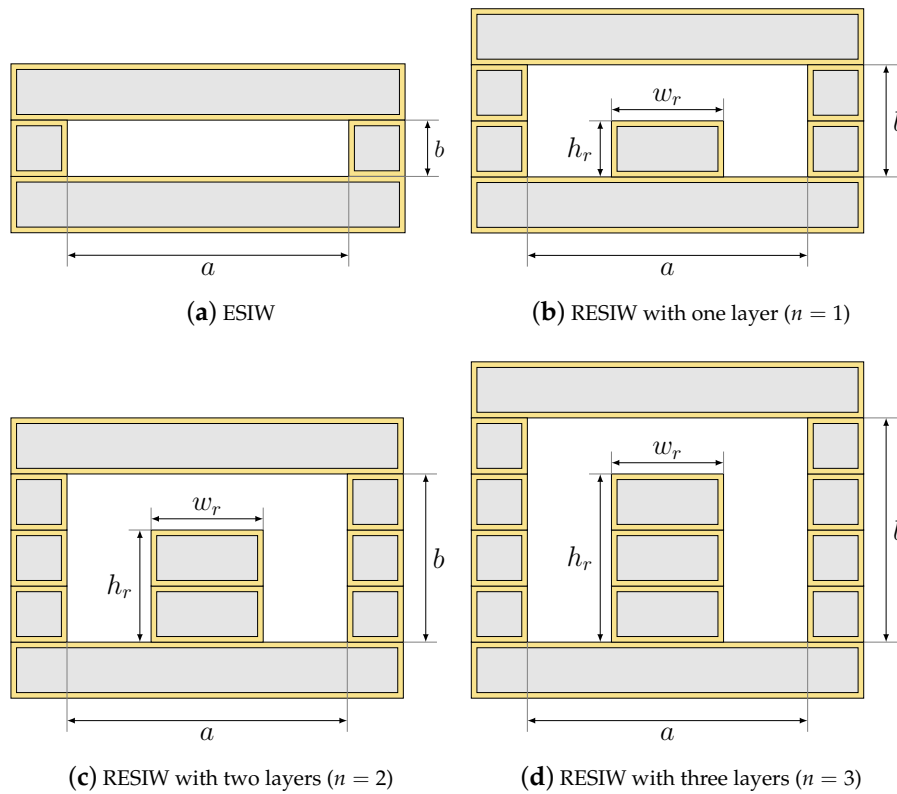
(a) ESIW

(b) RESIW with one layer ($n = 1$)

(c) RESIW with two layers ($n = 2$)

(d) RESIW with three layers ($n = 3$)

Figure A1. Cross sectional view of the ESIW and the ridge ESIW with different number of layers.

In the ridge waveguide, the cutoff frequencies of the fundamental mode TE_{10} (f_{c10}) and the first higher order mode TE_{20} (f_{c20}) can be obtained by solving the following transcendental equations [22],

$$\cot\left(\frac{2\pi f_{c_{10}}\left(\frac{a-w_r}{2}\right)}{c}\right) - \frac{b}{d}\tan\left(\frac{\pi w_r f_{c_{10}}}{c}\right) - \frac{B}{Y_{01}} = 0 \tag{A1}$$

$$\cot\left(\frac{2\pi f_{c_{20}}\left(\frac{a-w_r}{2}\right)}{c}\right) + \frac{b}{d}\cot\left(\frac{\pi w_r f_{c_{20}}}{c}\right) - \frac{B}{Y_{01}} = 0 \tag{A2}$$

where c is the light velocity; a and b are the width and height of the waveguide, respectively; and $d = b - h_r$ is the distance between the top ridge layer and top wall of waveguide (see Figure 1). The term B/Y_{01} is the susceptance that models the gap, and can be approximated as [17]

$$\frac{B}{Y_{01}} \approx 4\left(\frac{b}{d}\right)\left(\frac{af_c}{c}\right)\ln\csc\left(\frac{\pi d}{2b}\right) \tag{A3}$$

where f_c is f_{c10} for solving Equation (A1) and f_{c20} for solving Equation (A2).

Equations (A1) and (A2) can be used to obtain f_{c10} and f_{c20} as a function of the width of the ridge, w_r, which is the only design parameter in a RESIW that we can use in order to maximize the usable bandwidth ($f_{c20} - f_{c10}$). Figure A2 shows both cutoff frequencies f_{c10} and f_{c20} as a function of w_r for a RESIW manufactured with Rogers 4003C substrates of height $h = 0.813$ mm, permittivity $\epsilon_r = 3.66$ and width $a = 15.7988$ mm. The cutoff frequencies were computed both analytically with Equations (A1) and (A2) and numerically with the commercial software Computer Simulation Technology (CST). The results are shown for a RESIW with one, two and three ridge layers ($n = 1$, 2 and 3), and they are compared with the cutoff frequencies of an ESIW (no ridge layers).
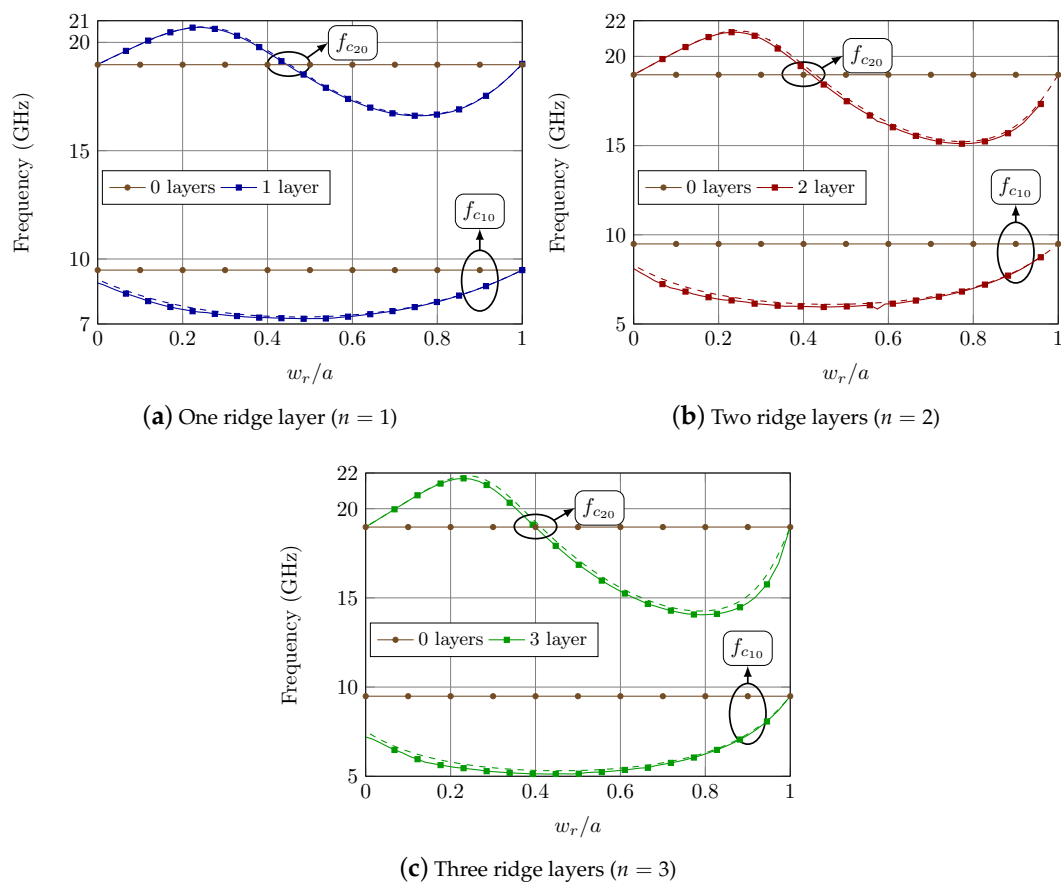
(**a**) One ridge layer ($n = 1$)

(**b**) Two ridge layers ($n = 2$)

(**c**) Three ridge layers ($n = 3$)

Figure A2. Cutoff frequencies of the fundamental and first higher order mode of a ridge ESIW with one, two and three ridge layers as a function of the ridge width w_r. Comparison between analytical (dashed lines) and simulated (continuous lines) results and comparison with an ESIW without any ridge layer.

It can be observed, in the first place, that there is a very good agreement between analytical and simulated results, which validates the accuracy of Equations (A1) and (A2). Besides, it can be concluded that the higher bandwidth (maximum distance between f_{c10} and f_{c20}) is achieved with $w_r/a \simeq 0.28$. Using this value of w_r as a starting point, and after optimization, optimum values of w_r that maximize the bandwidth were obtained for the the RESIW with one, two, and three ridge layers, and the values of the cutoff frequencies for these optimum values of w_r are shown in Table A1.

Table A1. Cutoff frequencies and bandwidth of the RESIW as the number of ridge layers (n) increases.

n	f_{10}(GHz)	f_{20}(GHz)	BW(GHz)	BW Increase
0	9.480	18.970	9.490	-
1	7.530	20.660	13.130	38%
2	6.227	21.352	15.125	15%
3	5.420	21.692	16.272	7%

The results depicted in Table A1 show that the bandwidth increases with the number of ridge layers. Using one ridge layer increases the bandwidth by 38% compared with the ESIW with no ridge layer. However, using two ridge layers supposes an increase in the bandwidth of only a 15% when compared with one ridge layer. Using three ridge layers increases the bandwidth by 7% compared with two ridge layers. Taking into account that increasing the number of ridge layers increases the volume,

weight, cost, and manufacturing complexity, for most wideband applications, the best compromise between bandwidth and ease of manufacturing will be the use of one ridge layer.

To test whether the usable bandwidth of the RESIW with one ridge layer can still be improved by using other unconventional geometries, the trapezoidal and two rectangular ridge geometries shown in Figure A3 were also studied.
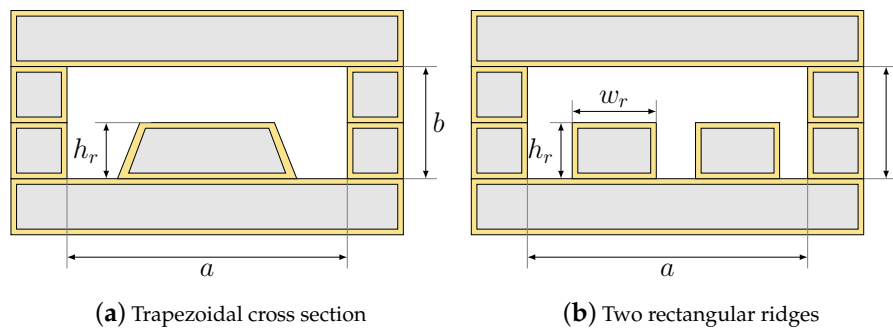

| **(a)** Trapezoidal cross section | **(b)** Two rectangular ridges |

Figure A3. Cross sectional view of the one layer ridge ESIW with unconventional geometries.

Table A2 shows the cutoff frequencies and the absolute bandwidth of these geometries compared with the rectangular cross section single layer ridge. It can be observed that a slightly higher bandwidth can be achieved with the trapezoidal geometry, but the improvement is so small that it is not worth complicating the manufacturing process.

Table A2. Cutoff frequencies and bandwidth for RESIW with on ridge layer and different ridge geometries.

Ridge Geometry	f_{10}(GHz)	f_{20}(GHz)	*BW*(GHz)
One rectangular ridge	7.530	20.660	13.130
One trapezoidal ridge	7.710	20.860	13.150
Two rectangular ridges	7.650	19.950	12.300

References

1. Deslandes, D.; Wu, K. Integrated microstrip and rectangular waveguide in planar form. *IEEE Microw. Wirel. Compon. Lett.* **2001**, *11*, 68–70. [CrossRef]
2. Belenguer, A.; Esteban, H.; Boria, V. Novel Empty Substrate Integrated Waveguide for High-Performance Microwave Integrated Circuits. *IEEE Trans. Microw. Theory Tech.* **2014**, *62*, 832–839. [CrossRef]
3. Martinez, J.A.; de Dios, J.J.; Belenguer, A.; Esteban, H.; Boria, V.E. Integration of a Very High Quality Factor Filter in Empty Substrate-Integrated Waveguide at *Q*-Band. *IEEE Microw. Wirel. Compon. Lett.* **2018**, *28*, 503–505. [CrossRef]
4. Belenguer, A.; Esteban, H.; Borja, A.L.; Boria, V.E. Empty SIW technologies: A major step toward realizing low-cost and low-loss microwave circuits. *IEEE Microw. Mag.* **2019**, *20*, 24–45. [CrossRef]
5. Mateo, J.; Torres, A.; Belenguer, A.; Borja, A. Highly Efficient and Well-Matched Empty Substrate Integrated Waveguide H-plane Horn Antenna. *IEEE Antennas Wirel. Propag. Lett.* **2016**, *15*, 1510–1513. [CrossRef]
6. Miralles, E.; Belenguer, A.; Mateo, J.; Torres, A.; Esteban, H.; Borja, A.; Boria, V. Slotted ESIW antenna with high efficiency for a MIMO radar sensor. *Radio Sci.* **2018**, *53*, 605–610. [CrossRef]
7. Khan, Z.U.; Alomainy, A.; Loh, T.H. Empty Substrate Integrated Waveguide Planar Slot Antenna Array for 5G Wireless Systems. In Proceedings of the 2019 IEEE International Symposium on Antennas and Propagation and USNC-URSI Radio Science Meeting, Atlanta, GA, USA, 7–12 July 2019; pp. 1417–1418.
8. Fernandez, M.D.; Ballesteros, J.A.; Belenguer, A. Design of a hybrid directional coupler in empty substrate integrated waveguide (ESIW). *IEEE Microw. Wirel. Compon. Lett.* **2015**, *25*, 796–798. [CrossRef]
9. Martinez, L.; Laur, V.; Borja, A.L.; Quéffélec, P.; Belenguer, A. Low Loss Ferrite Y-Junction Circulator Based on Empty Substrate Integrated Coaxial Line at Ku-Band. *IEEE Access* **2019**, *7*, 104789–104796. [CrossRef]

10. Peng, H.; Xia, X.; Ovidiu Tatu, S.; Xu, K.D.; Dong, J.; Yang, T. Broadband phase shifters using comprehensive compensation method. *Microw. Opt. Technol. Lett.* **2017**, *59*, 766–770. [CrossRef]

11. Esteban, H.; Belenguer, A.; Sánchez, J.R.; Bachiller, C.; Boria, V.E. Improved low reflection transition from microstrip line to empty substrate-integrated waveguide. *IEEE Microw. Wirel. Compon. Lett.* **2017**, *27*, 685–687. [CrossRef]

12. Liu, Z.; Xu, J.; Wang, W. Wideband Transition From Microstrip Line-to-Empty Substrate-Integrated Waveguide Without Sharp Dielectric Taper. *IEEE Microw. Wirel. Compon. Lett.* **2019**, *29*, 20–22. [CrossRef]

13. Belenguer, A.; Ballesteros, J.A.; Fernandez, M.D.; González, H.E.; Boria, V.E. Versatile, Error-Tolerant, and Easy to Manufacture Through-Wire Microstrip-to-ESIW Transition. *IEEE Trans. Microw. Theory Tech.* **2020**, *68*, 2243–2250. [CrossRef]

14. Liu, Z.; Wang, W.; Sun, D.; Deng, J.Y. Wideband microstrip-to-air-filled substrate integrated waveguide transition with controllable band-pass performance. *Microw. Opt. Technol. Lett.* **2020**, *62*, 3458–3462. [CrossRef]

15. Murad, N.; Lancaster, M.; Wang, Y.; Ke, M. Micromachined rectangular coaxial line to ridge waveguide transition. In Proceedings of the 2009 IEEE 10th Annual Wireless and Microwave Technology Conference, Clearwater, FL, USA, 20–21 April 2009; pp. 1–5.

16. Herraiz, D.; Esteban, H.; Martínez, J.A.; Belenguer, A.; Boria, V. Microstrip to Ridge Empty Substrate-Integrated Waveguide Transition for Broadband Microwave Applications. *IEEE Microw. Wirel. Compon. Lett.* **2020**, *30*, 257–260. [CrossRef]

17. Marcuvitz, N. *Waveguide Handbook*; MacGraw Hill: London, UK, 1951.

18. Helszajn, J. *Ridge Waveguides and Passive MicrowaveComponents*; Number 49 of IET Electromagnetic Waves Series; IET Digital Library: London, UK, 2000.

19. Cohn, S.B. Properties of ridge wave guide. *Proc. IRE* **1947**, *35*, 783–788. [CrossRef]

20. Cogollos, S.; Vague, J.; Boria, V.E.; Martínez, J.D. Novel planar and waveguide implementations of impedance matching networks based on tapered lines using generalized superellipses. *IEEE Trans. Microw. Theory Tech.* **2018**, *66*, 1874–1884. [CrossRef]

21. Gardner, M. *Mathematical Carnival*; American Mathematical Society: Providence, RI, USA, 1965

22. Hopfer, S. The design of ridged waveguides. *IRE Trans. Microw. Theory Tech.* **1955**, *3*, 20–29. [CrossRef]